Available online at
https://journal.uitm.edu.my/ojs/index.php/MJCET

e-ISSN: 2682-8588

Malaysian Journal of Chemical Engineering and Technology 8(2) 2025, 168–179

Malaysian Journal of Chemical Engineering and Technology

HF-free dry gel synthesis of MIL-100(Fe) for adsorptive removal of salicylic acid in wastewater treatment

Wan Nuraishah Wan Ishak[1], Nurul Syafiqah Mohd Sabri[2], Ying Pei Lim[3*], Huey Ling Tan[4]

[1,2,3,4]*Faculty of Chemical Engineering, Universiti Teknologi MARA, 40450 Shah Alam, Selangor, Malaysia*

ARTICLE INFO

Article history:
Received 04 February 2025
Revised 22 October 2025
Accepted 29 October 2025
Online first
Published 31 December 2025

Keywords:
Adsorption
Dry gel conversion
MIL-100(Fe)
Salicylic acid
Wastewater treatment

DOI:
10.24191/mjcet.v8i2.5013

ABSTRACT

This study reports an HF-free dry-gel conversion route to synthesise MIL-100(Fe) and evaluate its performance for adsorptive removal of salicylic acid from wastewater. Comprehensive characterisation of the material was conducted using XRD, FT-IR, FESEM and zeta potential. The dry gel conversion method successfully produced MIL-100(Fe) with an amorphous structure with an average particle size of 27 µm. Adsorption experiments achieved a maximum salicylic acid removal efficiency of 82.62% across the tested range (10 to 50 µg/mL), corresponding to an adsorption capacity of 80.93 mg/g at 120 minutes. Significant reductions in FT-IR peaks associated with carboxylic acid O–H stretching vibrations were observed, particularly in regions 3600 to 4000 cm^{-1} and 2500 to 3600 cm^{-1}. These changes indicate strong interactions between the carboxyl groups of salicylic acid and the active sites on the MIL-100(Fe) surface, confirming effective adsorption and removal of salicylic acid. These findings demonstrate that MIL-100(Fe) synthesised through a hydrofluoric acid-free dry gel conversion route is an effective and environmentally benign adsorbent for the removal of pharmaceutical pollutants from wastewater.

1. INTRODUCTION

Pharmaceutical and personal care products (PPCPs) constitute a major subgroup of emerging contaminants frequently detected in environmental matrices at trace concentrations, typically within the microgram per litre (µg·L^{-1}) or nanogram per litre (ng·L^{-1}) range (Ślósarczyk et al., 2021). Globally, more than 50,000 PPCP formulations are currently manufactured, with an estimated annual consumption exceeding 30 million tonnes (Chakraborty et al., 2023). Among these, salicylic acid (SA) is widely utilised in pharmaceuticals, cosmetics, and the chemical industry. Its persistence in aquatic environments arises from

[3*]Corresponding author. *E-mail address*: yingpei@uitm.edu.my
https://doi.org/10.24191/mjcet.v8i2.5013

the electron-withdrawing carboxyl group attached to the benzene ring, which confers strong resistance to microbial degradation (He et al., 2015). Reported SA concentrations in raw and treated wastewater across Asia range from 167 to 16,900 $ng \cdot L^{-1}$ (0.167–16.9 $\mu g \cdot L^{-1}$), classifying it within the non-steroidal anti-inflammatory drug (NSAID) group (Tran et al., 2018). In Europe, similar levels have been detected, with SA concentrations in urban wastewater in Spain ranging from <1.05 to 33.58 ± 19.68 $\mu g \cdot L^{-1}$ (Hijosa-Valsero et al., 2011).

The improper disposal of pharmaceuticals and personal care products (PPCPs) has become an escalating environmental concern due to the accumulation of toxic residues in wastewater during treatment. Many common used PPCPs including analgesics, anti-inflammatory drugs, antiepileptics, and psychostimulants are chemically stable and poorly removed by conventional treatment systems (Rojas & Horcajada, 2020). As a result, trace quantities of these substances persist in effluents, contributing to long-term contamination of aquatic environments. The release of such inadequately treated wastewater can disrupt aquatic ecosystems, induce bioaccumulation through the food web, and raise risks of chronic exposure for higher organisms.

Chlorination, one of the most prevalent disinfection methods, is insufficient for emerging contaminants. Although chlorine is widely used as an oxidant and disinfectant, its reactions with organic compounds generate undesirable by-products such as chlorate, chlorite, haloacetamides, and halomethanes. These compounds are known for their mutagenic and carcinogenic properties (Rojas & Horcajada, 2020). The associated health and ecological implications have accelerated research toward more sustainable and selective treatment alternatives. Among these, adsorption has gained significant attention as a low-energy, simple, and economically viable process capable of efficiently separating contaminants from aqueous systems. This is because PPCPs are often non-biodegradable, they can accumulate in aquatic organisms over time even at low concentrations, causing long-term toxicological effects (Luo et al., 2019). Certain compounds progressively concentrate through trophic transfer, exposing top predators and eventually humans to potentially harmful levels. Human exposure can occur indirectly through the consumption of contaminated aquatic organisms or crops irrigated with polluted water (Daginnus et al., 2011). Salicylic acid (SA), a typical PPCP compound widely utilised in pharmaceuticals and cosmetics, exemplifies this persistence. Its aromatic ring containing an electron-withdrawing carboxyl group enhances stability and limits biodegradability, leading to its continuous accumulation in wastewater streams (He et al., 2015).

Traditional wastewater treatment plants are primarily engineered to remove organic matter, nutrients, and microbial pathogens. Their standard operational stages physical separation, biological oxidation, and disinfection are generally inadequate for degrading or retaining micropollutants such as PPCPs (Li et al., 2021). Consequently, advanced treatment approaches have been developed to address this limitation, including membrane filtration, ozonation, advanced oxidation processes, adsorption, and bioaugmentation (Sartori et al., 2023). Among these, adsorption remains particularly attractive due to its operational simplicity, scalability, and low cost. Recent investigations highlight the potential of metal-organic frameworks (MOFs) as next-generation adsorbents for PPCP removal. MOFs possess exceptionally high surface areas, adjustable pore structures, and tunable chemical functionalities, allowing for efficient adsorption of complex organic molecules (Rojas & Horcajada, 2020). One of the most notable examples, MIL-100(Fe) also known as iron(III) trimesate has demonstrated remarkable capacity for capturing PPCPs from aqueous media due to its open metal sites and robust framework stability(Muñoz-Senmache et al., 2020).

https://doi.org/10.24191/mjcet.v8i2.5013

MIL-100(Fe) can be synthesised by several methods, with hydrothermal synthesis being the most widely reported. This approach typically produces highly crystalline materials but requires high temperature, long reaction times (Taherzade et al., 2022) and in many cases, the use of hazardous hydrofluoric acid (HF) as a mineralizing agent (Luo et al., 2019). Additionally, the product yield of MIL-100(Fe) obtained hydrothermally is relatively low at 76% at 160 °C. The dry gel conversion (DGC) method achieves a higher yield of 85% at the lower temperature of 140 °C (Luo et al., 2019). DGC method offers other distinct advantages including reduced solvent consumption and elimination of HF. These factors make the synthesis route both safer and more environmentally sustainable (Idrees et al., 2025). The combined benefits also translate into lower production cost and improved scalability. Given these benefits, the DGC route was selected in this study for the preparation of MIL-100(Fe).

Previous study by Luo et al., (2019) explored MIL-100(Fe) synthesised via DCG for applications like water vapor adsorption and desorption. However, limited attention has been given to its potential in removing emerging contaminants from wastewater. In one study, MIL-100(Fe) composites (e.g. MIL-100(Fe)$^{+}$ cellulose) have been used to remove pharmaceuticals like lorazepam (Taherzade et al., 2022). Salicylic acid, a pharmaceutical contaminant, is less studies compared to well-explored ones like carbamazepine, caffeine and ibuprofen (Zhi et al, 2024, Sivanesan et al, 2024, Siyal et al, 2025). This study aims to apply the greener method to evaluate the adsorption performance of MIL-100(Fe) for the removal of salicylic acid. This research offers practical insights into improving the sustainability and effectiveness of wastewater treatment while providing eco-friendly solution for mitigating the environmental impact of PPCPs.

2. METHODOLOGY

2.1 Materials

Iron nitrate nonahydrate ($Fe(NO_3)_3 \cdot 9H_2O$, 99%) was obtained from Bendosen Laboratory Chemicals, 2-methylimidazole ($C_4H_6N_2$, 99%) from Sigma-Aldrich, ethanol (C_2H_6O, 99%) from Chemiz, methanol (CH_3OH, 99%) from HmbG, pure salicylic acid powder from Take It Global Sdn Bhd. All chemicals were of analytical grade and used directly without further purification.

2.2 Method

Synthesis of MIL-100(Fe)

Following the procedure previously reported by Luo et al., (2019), MIL-100(Fe) was synthesised via dry gel conversion (DGC). Fe $(NO_3)_3 \cdot 9H_2O$ (4.0 g) was dissolved in 224 mL of deionised water, and 2-methylimidazole (2.6 g) as the organic linker was added to the solution (Perera et al., 2019). The solution was stirred at 400 rpm for 3 h at room temperature, followed by freeze-drying for 5 days to obtain an orange solid. The dried powder was ground for 5 min and conditioned in a humidity chamber (60% RH, 1 h) at room temperature. The pretreated powder was then transferred to a Teflon-lined autoclave and crystallised at 160 °C for 24 h. The resulting product was repeatedly washed with deionised water and ethanol until the filtrate became clear, then filtered and dried at 120 °C for 12 h. The process yielded approximately 2.5 g of MIL-100(Fe) as a crystalline orange powder.

https://doi.org/10.24191/mjcet.v8i2.5013

Characterisation

The structural characterisation and phase identification of the synthesised MIL-100(Fe) were performed using powder X-ray diffraction (XRD) on a Rigaku D/Max-2200V/PC diffractometer operated at 40 kV and 44 mA. The diffraction patterns were recorded over a 2θ range of 2° to 80° with a scanning rate of 2°/min. The surface morphology and elemental composition of the adsorbent were examined using field emission scanning electron microscopy (FESEM, JEOL JSM-7600F) at magnifications of 5,000× and 10,000×. Prior to imaging, the sample was sputter-coated with a thin layer of platinum using an Auto Fine Coater (JFC-1600) to enhance conductivity. Particle size measurements were determined from the FESEM micrographs using ImageJ software to obtain representative size distributions. For compositional analysis, Fourier Transform InfraRed (FT-IR) spectroscopy (Perkin Elmer/Spectrum One) was employed. Measurements were taken with 4 scans in the wavenumber range of 515 to 4000 cm^{-1} for both the adsorbent and the adsorbate (salicylic acid solution). Zeta potential measurements were carried out to assess the surface charge of the synthesised adsorbent using a Zetasizer (Malvern NanoZS). Before the measurement, the MIL-100(Fe) sample was sonicated using an ultrasonic bath (Grant XUBA 1) to ensure proper dispersion.

Adsorption study

A standard curve was created by dissolving 0.05 g of salicylic acid powder in methanol. The solution was transferred to a 1000 mL volumetric flask, and methanol was added until the calibration mark was reached, producing a standard solution with a concentration of 50 µg/mL salicylic acid. Using this stock solution, five different concentrations ranging from 10 to 50 µg/mL were prepared through serial dilution. The absorbance of these samples were measured using UV-Vis spectroscopy (Agilent Technologies) at a wavelength of 300 nm (Ashara & Shah, 2017). A standard curve plotting the absorbance against salicylic acid concentration was then constructed. Next, 10 mg of MIL-100(Fe) was mixed with 100 mL of 50 µg/mL salicylic acid (SA) standard solution in a beaker to investigate the effects of adsorption time and SA concentration. The mixture was stirred intermittently at 5 minutes for the first 30 minutes, 10 minutes intervals for the next 30 minutes and 15 minutes intervals for the remaining hour, totaling 2 hours of mixing at room temperature. The sample was then centrifuged at 1400 rpm for 5 minutes and the supernatant was collected. The absorbance of the supernatant was measured using UV-is spectroscopy to determine salicylic acid concentration via the calibration curve method. This procedure was repeated with MIL-100(Fe) dosages of 20, 30, 40, and 50 mg. Once the optimal dosage was identified, the experiment was repeated using salicylic acid concentrations of 10, 20, 30, and 40 µg/mL, maintaining the same stirring intervals as previously described. The efficiency of MIL-100(Fe) was reported using removal percentage and adsorption capacity, q. Adsorption rate is a kinetic parameter that reflects the speed of SA uptake while the removal percentage is a static parameter that reflects the extent of SA uptake once equilibrium is reached. The removal percentage and the adsorption capacity, q (µg/g) were calculated using the following equations: where C_o (µg/mL) and C_f (µg/mL) are the initial and final concentrations of salicylic acid, V is solution volume (mL), and W is the mass of MIL-100(Fe) (g).

$$\text{Removal } (\%) = \frac{C_o - C_f}{C_o} \times 100\% \quad (1)$$

https://doi.org/10.24191/mjcet.v8i2.5013

$$q=\frac{(C_o - C_t)V}{W} \quad (2)$$

3. RESULTS AND DISCUSSION

Fig.1 shows the x-ray diffraction (XRD) patterns of MIL-100(Fe) synthesised via the dry gel conversion method. The broad dispersion peaks observed at 34°, 34.4°, 62.45°, and 62.5° 2θ confirmed the formation of a semi-amorphous structure and consistent with literature data for unheated MIL-100(Fe), which exhibits a semi-amorphous structure when prepared using similar method (Luo et al., 2019). Amorphous structures are characterised by their disordered arrangement and broader pore sizes compared to crystalline forms, providing multiple selectivity. This structural property enables the adsorbent to capture molecules of various sizes, enhancing its effectiveness in removing a range of pollutants from wastewater.

SEM images (Fig.2) revealed irregular shapes and non-faceted particles, indicating a lack of crystalline morphology and appeared as large aggregates with an average size of 27 μm (Fig. 2c). HF-free synthesis of MIL-100(Fe) tend to produce large aggregates with broad particle size distributions (0.4 to 10 μm) (Sobhani et al., 2024, Idrees et al., 2025) owing to the absence of modulating agent such as fluorides. Under these conditions, nucleation is less controlled and crystal growth proceeds without sufficient constraints, leading to the formation of clustered aggregates. Smaller particle sizes facilitate faster diffusion by reducing the distance adsorbate molecules need to travel to reach adsorption sites. Consequently, larger aggregates in this study led to a slower adsorption rate, achieving 82.16% removal in 120 minutes, compared to 93% removal in just 5 mins reported in the work by Sobhani et al., (2024).

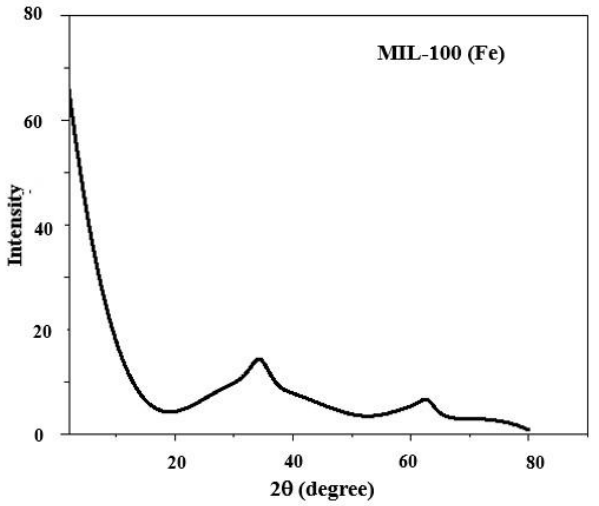

Fig.1. XRD pattern of MIL-100(Fe) with broad peak at 34, 34.4, 62.45, and 62.5 of 2θ° indicating amorphous structure

Source: Author's own data

https://doi.org/10.24191/mjcet.v8i2.5013

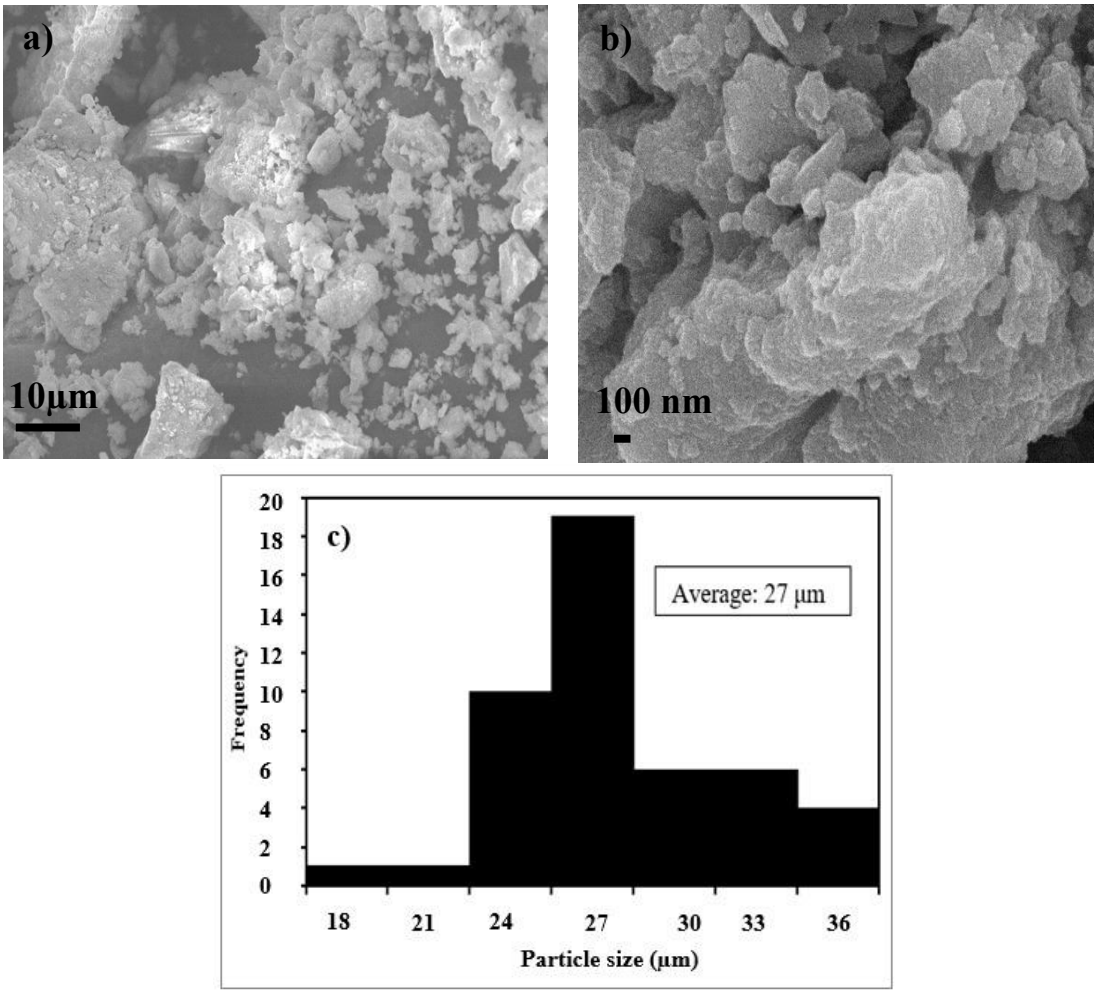

Fig. 2. SEM images of MIL-100(Fe) at magnifications of a)1,300× and b) 3,000× reveal its amorphous structure; c) MIL-100(Fe) appears as large aggregates with an average size of 27 µm

Source: Author's own data

Zeta potential is a key indicator of the strength of electrostatic interactions and colloidal stability. The synthesised MIL-100(Fe) shows a zeta potential of −16.8 mV (Fig.3a), indicating its stability. Particles with zeta potential values below −15mV or above +15mV are typically considered stable due to electrostatic repulsion (White et al., 2007). In contrast, salicylic acid nanoparticles carry a positive charge of +3.99 mV (Abdel-Rahman et al., 2021). This charge disparity facilitates electrostatic attraction between the two. When the positively charged salicylic acid interacts with negatively charged MIL-100(Fe) surface, the opposite charges align, resulting in a strong electrostatic bond. This interaction significantly enhances the adsorption capacity of MIL-100(Fe) for salicylic acid molecules.

https://doi.org/10.24191/mjcet.v8i2.5013

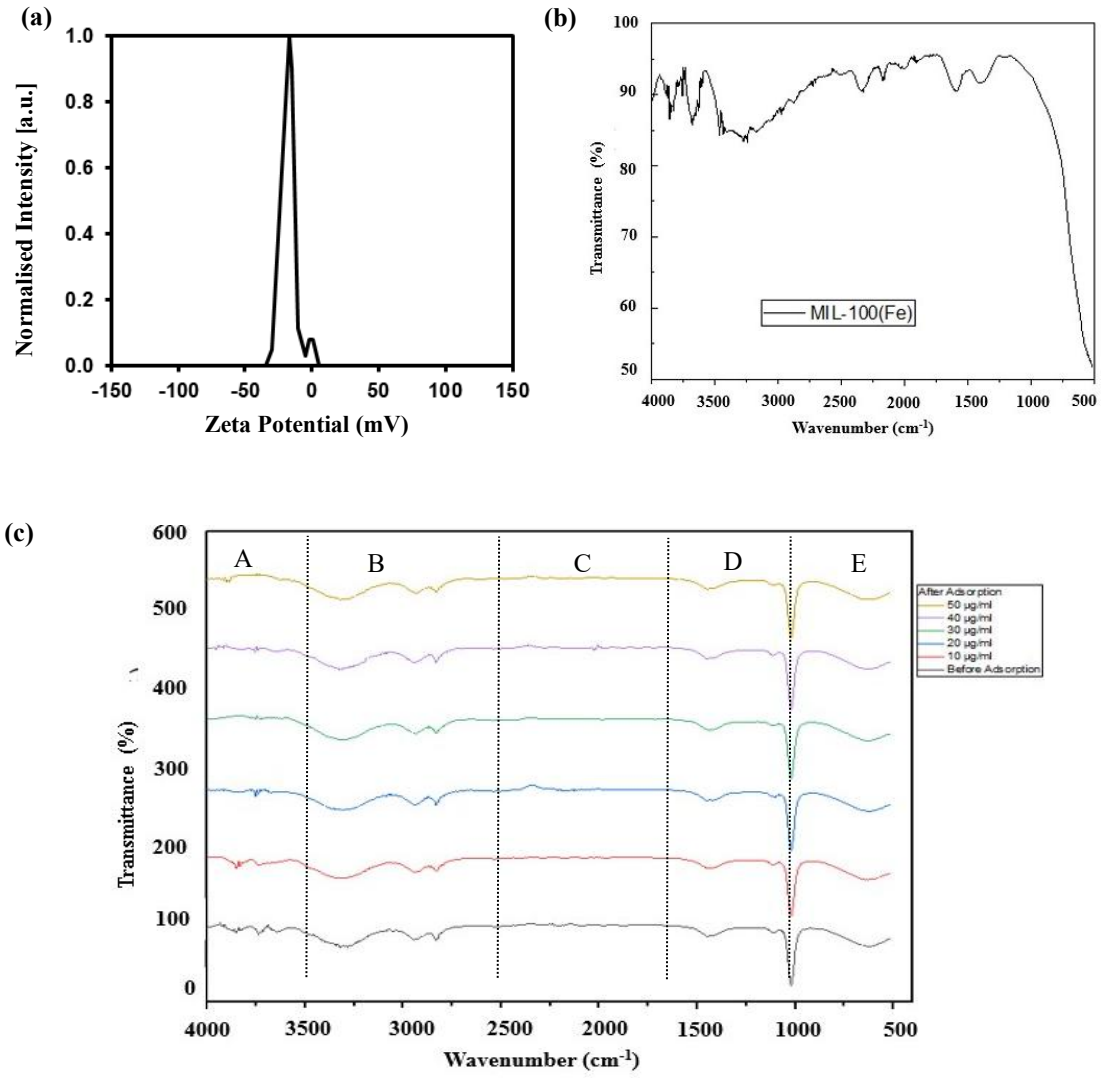

Fig .3. (a) Zeta potential distribution curve for MIL-100(Fe), (b) FTIR spectrum of MIL-100(Fe), (c) FTIR spectra of MIL-100(Fe) before adsorption (black line), after adsorption (coloured line) for salicylic acid at concentrations of 10, 20, 30, 40, and 50 µg/mL, recorded following 120 minutes of interaction at room temperature

Source: Author's own data

The FTIR spectrum in Fig.3b reveals peaks at 3858 cm^{-1} (O–H), 3680 cm^{-1} (O–H), 3464 cm^{-1} (N–H stretching), 3244 cm^{-1} (O–H stretch), 2327 cm^{-1} (C–N), 2173 cm^{-1} (C=O stretching) and 1586 cm^{-1} (N–H), indicating the presence of diverse functional groups on the MIL-100(Fe) surface. These functional groups provide different binding sites with varying affinities, enhancing the adsorption capacity and selectivity of the material. The FTIR analysis of salicylic acid at varying concentrations (10, 20, 30, 40, and 50 µg/mL) shows a reduction in peaks, particularly in region A (3600 to 4000 cm^{-1}) and B (2500 to 3600 cm^{-1}) in Fig. 3c. These reductions correspond to the O–H stretching vibrations of alcohol

https://doi.org/10.24191/mjcet.v8i2.5013

and carboxylic acid groups, confirming that MIL-100(Fe) effectively removes salicylic acid in solution. Additionally, a new peak around 2000 cm^{-1} at a concentration of 40 μg/mL suggests the formation of a C=O stretch (carboxylate), likely resulting from the adsorbed CO_2 species on MIL-100(Fe) precursors, ($Fe(NO_3)_3 \cdot 9H_2O$) and 2-methylimidazole ($C_4H_6N_2$). In region E, slight reductions in peaks between 1023 to 620 cm^{-1}, corresponding to C–O stretch (primary alcohol) and C=C bend (alkene in benzene ring), further support successful adsorption of salicylic acid on the active sites of MIL-100(Fe). The spectral changes confirm that the adsorbent actively reduces the concentration of salicylic acid in solution, underscore the capability of MIL-100(Fe) to remove salicylic acid effectively.

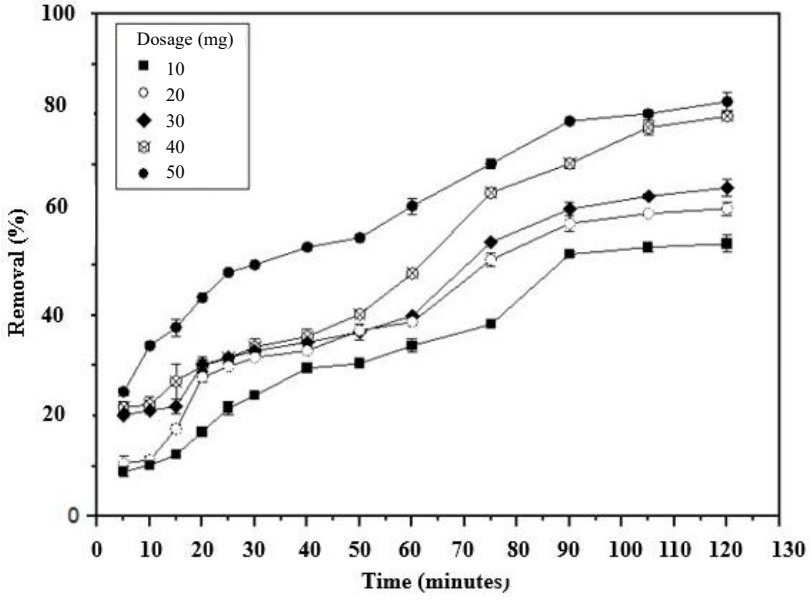

Fig.4. The removal percentage at varying dosages of MIL-100(Fe) demonstrate a positive correlation, with the removal efficiency increasing as the dosage amount is raised

Source: Author's own data

Fig.4 illustrates the relationship between MIL-100(Fe) dosage (mg) and adsorption time (minutes), showing a sharp initial decline in salicylic acid concentration. The rapid uptake observed at the early-stage results from a high concentration gradient between the solute and the adsorbent surface, which promotes the immediate occupation of active sites on MIL-100(Fe). As adsorption continues, the rate progressively decreases due to the gradual saturation of available binding sites. When the surface becomes nearly occupied, the process slows until equilibrium is attained. At this equilibrium state, the rates of adsorption and desorption become identical, and the distribution of salicylic acid molecules between the solution and the adsorbent surface remains constant, signifying that the adsorption process has stabilised.

https://doi.org/10.24191/mjcet.v8i2.5013

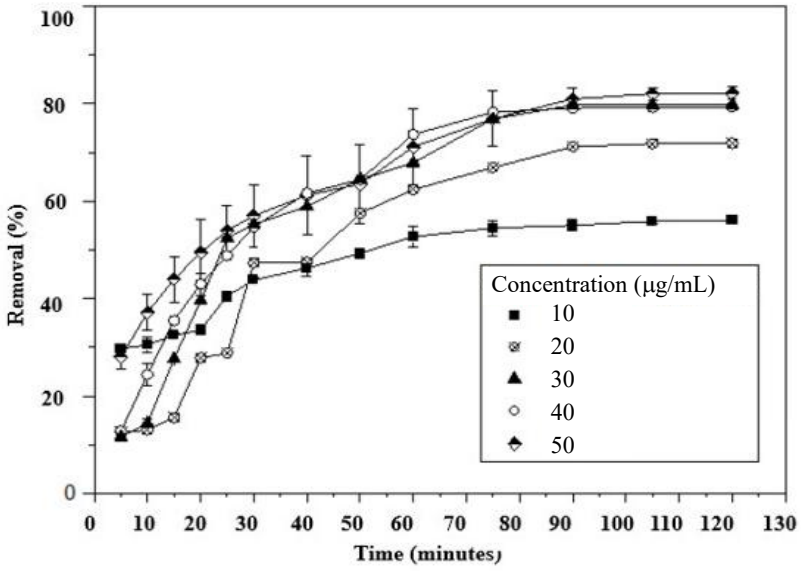

Fig.5. Removal percentage at different concentration of MIL-salicylic acid indicates that as the concentration increases, the removal percentage also rises

Source: Author's own data

Figure 5 shows that higher SA concentrations at a fixed 50 mg MIL-100(Fe) dosage require longer times to reach equilibrium due to increased adsorbate load. However, the initial removal rate (µg/mL·min) is faster at higher concentrations of salicylic acid than those in lower concentrations, driven by a stronger mass transfer gradient. The DCG-synthesised MIL-100(Fe) achieved 82.62% removal and 80.93 mg/g capacity in 120 minutes, compared to nearly 100% removal for carbamazepine, caffeine, and ibuprofen using hydrothermal MIL-100(Fe) composites (0.2–0.6 µm) in aqueous matrices (Muñoz-Senmache et al., 2020). The lower efficiency here is likely due to larger particle size (27 µm) reducing surface area and the methanol matrix altering SA solubility compared to water. Additionally, Duan et al., (2016) reported equilibrium for dyes (rhodamine 6G (R6G), rhodamine B (RB) and reactive red (RR)) in 15–20 minutes using nanoscale MIL-100(Fe) synthesised without HF but with ethanol, which reduces solvent polarity and enhances ligand deprotonation, improving morphology and efficiency. Direct comparisons are limited by differences in contaminant chemistry (SA vs dyes), particle sizes and solvent (methanol vs ethanol/ water).

Compared to hydrothermal synthesis, DGC offers distinct advantages. It eliminates HF, enhancing safety and reducing environmental risks. DGC also achieves higher yields (85% at 140 °C vs 76% at 160 °C for hydrothermal (Luo et al., 2019). Cost benefits arise from lower energy requirements (freeze-drying vs high pressure heating) and minimal solvent use. However, the amorphous structure obtained through the dry gel conversion (DGC) method may compromise long-term structural stability compared to the crystalline MIL-100(Fe) produced via conventional hydrothermal synthesis. Despite this limitation, the broader pore distribution of the DGC-derived material enhances its ability to accommodate a wide range of pollutants, including salicylic acid. These trade-offs emphasise the DGC method's potential as a sustainable and economically viable strategy for wastewater treatment, particularly in addressing pharmaceutical contaminants.

https://doi.org/10.24191/mjcet.v8i2.5013

4. CONCLUSION

This study presents a sustainable and cost-efficient route for synthesizing MIL-100(Fe) using the dry gel conversion method for the removal of pharmaceutical pollutants, with salicylic acid selected as a model compound. The obtained MIL-100(Fe) exhibited an amorphous morphology with an average particle size of approximately 27 µm and a zeta potential of −16.8 mV, indicating good colloidal stability. Adsorption tests showed a removal efficiency of 82.6% and an adsorption capacity of 80.93 mg g^{-1} within 120 minutes at a dosage of 50 mg. Structural and surface analyses using XRD, FT-IR, and FESEM confirmed the successful formation of MIL-100(Fe) and its functional properties, while FT-IR spectra revealed a notable reduction in carboxylic acid peaks after adsorption, evidencing strong interactions between MIL-100(Fe) and salicylic acid molecules. Compared with conventional hydrothermal synthesis, the dry gel conversion approach eliminates the use of hazardous hydrofluoric acid and enhances both material yield and adsorption performance. These results demonstrate that MIL-100(Fe) is a promising, environmentally benign adsorbent for addressing emerging contaminants in wastewater.

ACKNOWLEDGEMENTS/FUNDING

The authors would like to express their sincere gratitude to the Faculty of Chemical Engineering, Universiti Teknologi MARA (UiTM) for the support in completing this study.

CONFLICT OF INTEREST STATEMENT

The authors declare no conflict interest.

AUTHORS' CONTRIBUTIONS

Wan Nuraishah Wan Ishak, Nurul Syafiqah Mohd Sabri: Methodology, formal analysis, investigation and writing-original draft; **Huey Ling Tan**: Methodology, and formal analysis, writing review, editing; **Lim Ying Pei**: Conceptualisation, formal analysis, and validation, writing-review.

REFERENCES

Abdel-Rahman, F. A., Khafagi, E. Y., Soliman, M. S., Shoala, T., & Ahmed, Y. (2021). Preharvest application of salicylic acid induces some resistant genes of sweet pepper against black mold disease. *European Journal of Plant Pathology*, *159*(4), 755–768. https://doi.org/10.1007/s10658-020-02199-z

Ashara, K. C., & Shah, K. V. (2017). Nuts and bolts of oil and temperature in topical preparations of salicylic acid. *Folia Medica*, *59*(3), 279–288. https://doi.org/10.1515/folmed-2017-0034

Chakraborty, A., Adhikary, S., Bhattacharya, S., Dutta, S., Chatterjee, S., Banerjee, D., Ganguly, A., & Rajak, P. (2023). Pharmaceuticals and personal care products as emerging environmental contaminants: Prevalence, toxicity, and remedial approaches. *ACS Chemical Health and Safety, 30*(6), 362–388. https://doi.org/10.1021/acs.chas.3c00071

Daginnus, K., Gottardo, S., Payá-Pérez, A., Whitehouse, P., Wilkinson, H., & Zaldívar, J. M. (2011). A model-based prioritisation exercise for the European Water Framework Directive. *International Journal of Environmental Research and Public Health*, *8*(2), 435–455. https://doi.org/10.3390/ijerph8020435

Duan, S., Li, J., Liu, X., Wang, Y., Zeng, S., Shao, D., & Hayat, T. (2016). HF-free synthesis of nanoscale metal-organic framework NMIL-100(Fe) as an efficient dye adsorbent. *ACS Sustainable Chemistry and Engineering*, *4*(6), 3368–3378. https://doi.org/10.1021/acssuschemeng.6b00434

He, Z., Meng, M., Yan, L., Zhu, W., Sun, F., Yan, Y., Liu, Y., & Liu, S. (2015). Fabrication of new cellulose acetate blend imprinted membrane assisted with ionic liquid ([BMIM]Cl) for selective adsorption of salicylic acid from industrial wastewater. *Separation and Purification Technology*, *145*, 63–74. https://doi.org/10.1016/j.seppur.2015.03.005

Hijosa-Valsero, M., Matamoros, V., Pedescoll, A., Martín-Villacorta, J., Bécares, E., García, J., & Bayona, J. M. (2011). Evaluation of primary treatment and loading regimes in the removal of pharmaceuticals and personal care products from urban wastewaters by subsurface-flow constructed wetlands. *International Journal of Environmental Analytical Chemistry*, *91*(7–8), 632–653. https://doi.org/10.1080/03067319.2010.526208

Idrees, M., Mastronardo, E., Piperopoulous, E., Milone, C., Calabrese, L. (2025). Impact of HF-free synthesis modification on purity and adsorption performance of MOF MIL-100(Fe) for gas capture and energy storage applications. *Applied Sciences*, *15*(11), 6097. https://doi.org/10.3390/app15116097

Li, W., Zhang, T., Lv, L., Chen, Y., Tang, W., & Tang, S. (2021). Room-temperature synthesis of MIL-100(Fe) and its adsorption performance for fluoride removal from water. *Colloids and Surfaces A: Physicochemical and Engineering Aspects, 624,* 126791. https://doi.org/10.1016/j.colsurfa.2021.126791

Luo, Y., Tan, B., Liang, X., Wang, S., Gao, X., Zhang, Z., & Fang, Y. (2019). Dry gel conversion synthesis of hierarchical porous MIL-100(Fe) and its water vapor adsorption/desorption performance. *Industrial and Engineering Chemistry Research*, *58*(19), 7801–7807. https://doi.org/10.1021/acs.iecr.9b01647

Muñoz-Senmache, J. C., Kim, S., Arrieta-Pérez, R. R., Park, C. M., Yoon, Y., & Hernández-Maldonado, A. J. (2020). Activated carbon–metal organic framework composite for the adsorption of contaminants of emerging concern from water. *ACS Applied Nano Materials*, *3*(3), 2928–2940. https://doi.org/10.1021/acsanm.0c00190

Rojas, S., & Horcajada, P. (2020). Metal-organic frameworks for the removal of emerging organic contaminants in water. *Chemical Reviews*, *120*(16), 8378–8415. https://doi.org/10.1021/acs.chemrev.9b00797

Sivanesan, J., Rameshwar S. S., Sivaprakash, B., Rajamohan, N., Osman, A. I., Al-Muhtasesb, A. (2024). Advanced methods for treating gemfibroil and carbamazepine in wastewater:A review, *Environmental Chemistry Letters*, *22*, 3171–3194. https://doi.org/10.1007/s10311-024-01765-9

Siyal, A. A., Mohamed R., Ahmad, F., Abdul Malek, M., Alsubih, M., Shamsuddin, R., Hussain, S., Musa, S. (2025) A review of the developments in adsorbents for the efficient adsorption of ibuprofen from wastewater, *RSC Advances, 15*, 17843–17861. https://doi.org/10.1039/D5RA02007G

Ślósarczyk, K., Jakóbczyk-Karpierz, S., Różkowski, J., & Witkowski, A. J. (2021). Occurrence of pharmaceuticals and personal care products in the water environment of Poland: A review. *Water (Switzerland)*, *13*(16). https://doi.org/10.3390/w13162283

Sobhani, D., Djahaniani, H., Duong, A., & Kazemian, H. (2024). Efficient removal of microcystin-LR from contaminated water using water-stable MIL-100(Fe) synthesized under HF-free conditions. *Environmental Science and Pollution Research*, *31*(16), 24512–24524. https://doi.org/10.1007/s11356-024-32675-6

Taherzade, S. D., Abbasichaleshtori, M., Soleimannejad, J. (2022). Efficient and ecofriendly cellulose-supported MIL-100(Fe) for wastewater treatment. *RSC Advances*, *12*, 9023-9035. https://doi.org/10.1039/D1RA08949H

https://doi.org/10.24191/mjcet.v8i2.5013

Tran, N. H., Reinhard, M., & Gin, K. Y. H. (2018). Occurrence and fate of emerging contaminants in municipal wastewater treatment plants from different geographical regions-a review. In *Water Research* (Vol. 133). Elsevier. https://doi.org/10.1016/j.watres.2017.12.029

White, B., Banerjee, S., Brien, S. O., Turro, N. J., & Herman, I. P. (2007). Zeta-potential measurements of surfactant-wrapped individual single-walled carbon nanotubes. *Journal of Physical Chemistry C, 2*(1), 13684–13690. https://doi.org/10.1021/jp070853e

Zhi, K., Xu, J., Li, S., Luo, L., Liu, D., Li, Z., Guo, L., Hou, J. (2024). Progress in the elimination of organic contaminants in wastewater by activation persulfate over iron-based metal-organic frameworks. *Nanomaterials (Basel)*, *14*(5), 473. https://doi.org/10.3390/nano14050473

https://doi.org/10.24191/mjcet.v8i2.5013